Bacteriorhodopsin's M_{412} Intermediate Contains a 13-*cis*,14-*s*-*trans*,15-*anti*-Retinal Schiff Base Chromophore†

James B. Ames,‡ Stephen P. A. Fodor,‡ Ronald Gebhard,§ Jan Raap,§ Ellen M. M. van den Berg,§ Johan Lugtenburg,§ and Richard A. Mathies*,‡

Department of Chemistry, University of California, Berkeley, California 94720, and Department of Chemistry, Leiden University, 2300 RA Leiden, The Netherlands

Received October 14, 1988; Revised Manuscript Received January 17, 1989

ABSTRACT: The structure of the retinal chromophore about the C=N and C_{14}—C_{15} bonds in bacteriorhodopsin's M_{412} intermediate has been determined by analyzing resonance Raman spectra of ^2H and ^{13}C isotopic derivatives. Normal mode calculations on 13-*cis*-retinal Schiff bases demonstrate that the C_{15}–D rock and N–C_{Lys} stretch are strongly coupled for C=N-syn chromophores and weakly coupled for C=N-anti chromophores. When the Schiff base geometry is anti, the C_{15}–D rock appears as a localized resonance Raman active mode at ~980 cm^{-1}, which is moderately sensitive to ^{13}C substitution at positions 14 and 15 (~7 cm^{-1}) and insensitive to ^{13}C substitution at the ϵ position of lysine. When the Schiff base geometry is syn, in-phase and out-of-phase combinations of the C_{15}–D rock and N–C_{Lys} stretch are predicted at ~1060 and ~910 cm^{-1}, respectively. The in-phase mode is more sensitive to ^{13}C substitution at positions 14 and 15 (~15 cm^{-1}) and at the ϵ position of lysine (~4 cm^{-1}). Calculations and comparison with experimental data on dark-adapted bacteriorhodopsin indicate that the in-phase mode at ~1060 cm^{-1} carries the majority of the resonance Raman intensity. M_{412} exhibits a C_{15}–D rock at 968 cm^{-1} that shifts 8 cm^{-1} when ^{13}C is added at positions 14 and 15 and is insensitive to ^{13}C substitution at the ϵ-position of lysine. This demonstrates that M_{412} contains a C=N-anti Schiff base. Time-resolved Raman experiments on M_{412} under a variety of conditions show that the various rise and decay components of M_{412} in the light-adapted photocycle all contain C=N-anti chromophores. Finally, M_{412} exhibits a 14,15-D_2 coupled rock at 958 cm^{-1} which shows that the chromophore has a 14-s-trans conformation. We conclude that M_{412} contains a 13-cis,14-s-trans,15-anti chromophore. This result supports the recently proposed C-T model for the mechanism of the proton pump in bacteriorhodopsin [Fodor, S. P. A., Ames, J. B., Gebhard, R., van den Berg, E. M. M., Stoeckenius, W., Lugtenburg, J., & Mathies, R. A. (1988) *Biochemistry 27*, 7097–7101].

Bacteriorhodopsin (BR),[1] the intrinsic membrane protein found in the purple membrane of *Halobacterium halobium*, contains an *all-trans*-retinal chromophore attached to Lys_{216} via a protonated Schiff base linkage (Stoeckenius & Bogomolni, 1982). BR utilizes light energy absorbed by its chromophore to transport protons across the bacterial cell membrane. Light absorption initiates a cyclic series of reactions called the photocycle: $BR_{568} \rightarrow J \rightarrow K \rightarrow L_{550} \rightarrow M_{412} \rightarrow N \rightarrow O_{640} \rightarrow BR_{568}$. The initial photochemical step ($BR_{568} \rightarrow J$) involves a femtosecond trans → cis torsional isomerization about the C_{13}=C_{14} bond (Mathies et al., 1988). The $J \rightarrow K$, $K \rightarrow L_{550}$, and $L_{550} \rightarrow M_{412}$ steps involve the relaxation of the 13-cis chromophore and protein structure and deprotonation of the Schiff base. The chromophore reprotonates during the $M_{412} \rightarrow N$ transition (Fodor et al., 1988b) and thermally reisomerizes back to all-trans during the formation of O_{640} (Smith et al., 1983). In the dark, BR_{568} converts to dark-adapted bacteriorhodopsin that contains a 2:1 mixture of 13-cis,15-syn and all-trans,15-anti protonated Schiff base chromophores denoted BR_{555} and BR_{568}, respectively (Scherrer et al., 1989).[2]

Models for the proton pump have been proposed in which a change in C_{14}—C_{15} conformation or C=N configuration occurs in the later part of the photocycle (Schulten & Tavan, 1978; Smith et al., 1986). These structural changes could serve as a "reprotonation switch" that changes the hydrogen-bonding connectivity of the Schiff base from the cell exterior to the cytoplasm. Recently we have demonstrated that L_{550} and N both contain 13-cis,14-s-trans,15-anti chromophores (Fodor et al., 1988a,b). These results argue against photocycle models invoking a chromophore-based reprotonation switch and led us to propose the C-T model for the mechanism of the proton pump (Fodor et al., 1988b). However, the structure of the chromophore in the intervening M_{412} intermediate has not been thoroughly characterized. Recent solid-state NMR experiments on M_{412} have isolated two forms of M_{412} at −40 °C and alkaline pH. A 13-cis,15-syn form was trapped in 0.2 M NaCl while a 13-cis,15-anti form was trapped in guanidine hydrochloride (Smith et al., 1989). To determine the form of M_{412} that participates in the light-adapted photocycle and to test the C-T model, we wanted to elucidate the structure of M_{412} using time-resolved methods at room temperature.

† Supported by the National Institutes of Health (GM 27057), the National Science Foundation (CHE 86-15093), the Netherlands Foundation for Chemical Research (SON), and the Netherlands Organization for the Advancement of Pure Research (NWO). S.P.A.F. is an NIH postdoctoral fellow (GM 11266).

* To whom correspondence should be addressed.
‡ University of California.
§ Leiden University.

[1] Abbreviations: BR, bacteriorhodopsin; PSB, protonated Schiff base; SB, Schiff base; HEPES, 4-(2-hydroxyethyl)-1-piperazineethanesulfonic acid.

[2] The absorption maximum of the 13-cis chromophore in dark-adapted bacteriorhodopsin is now estimated to be 555 nm (Scherrer et al., 1989). Therefore, we have changed the abbreviation for this component from BR_{548} to BR_{555}.

0006-2960/89/0428-3681$01.50/0

Resonance Raman spectroscopy is an effective method for determining the in situ structure of the retinal chromophore in bacteriorhodopsin. Extensive vibrational analyses on the retinal isomers and on the chromophore in BR_{568} and BR_{555} (Curry et al., 1985; Smith et al., 1987a,b) have provided tests for determining the C_{13}=C_{14} configuration (Smith et al., 1985a), the C_{14}—C_{15} conformation (Smith et al., 1986; Fodor et al., 1988a), and the C=N configuration in *protonated* Schiff bases (Smith et al., 1984). In this paper we present a new method for determining the C=N configuration of the *unprotonated* Schiff base chromophore found in M_{412}. This diagnostic makes use of the geometry-dependent coupling between the C_{15}–D rock and N–C_{lys} stretch. In the syn geometry these coordinates are strongly coupled, while in the anti geometry they are uncoupled. This causes the frequency and normal mode character of the C_{15}–D rocking mode to be characteristically sensitive to the Schiff base configuration. This method, together with those developed earlier, has allowed us to determine the complete structure of the retinal chromophore in M_{412}.

Materials and Methods

Sample Preparation. Cultures of *H. halobium* (ET 1001) were grown and the purple membrane was purified according to previously published procedures (Braiman & Mathies, 1980). Native purple membrane was bleached in 1 M NH_2OH at pH 7.8 in the dark for 12–14 h at 37 °C (Fodor et al., 1988a). The bleached membrane was then pelleted and washed with pH 7, 10 mM HEPES buffer three times to remove unreacted NH_2OH. The bleached membrane was titrated with aliquots of isotopically labeled *all-trans*-retinal dissolved in a minimum volume of ethanol. The regeneration was monitored by the absorbance increase at 568 nm. Excess retinal and residual oximes were removed by repeated washes in 2% fatty acid free bovine serum albumin until no detectable retinal oxime absorbance remained at 350 nm (~10 washes). Samples used in the Raman experiments consisted of purple membrane fragments suspended in 0.2 M NaCl (low salt) or 3 M KCl (high salt) with 10 mM phosphate at pH 7 or 10 mM borate at high pH. The *all-trans*-retinal isotopic derivatives (15-^{13}C; 14,15-^{13}C,15-D; 14,15-D_2; and 15-D) were synthesized according to previously published procedures (Pardoen et al., 1984). The [ε-^{13}C]lysine BR was prepared following the procedure of Argade et al. (1981). The isotopic purity was >98% for each deuterium derivative and >95% for the ^{13}C derivatives.

Raman Spectroscopy. Raman spectra of M_{412} were obtained by using a dual-beam flow apparatus (Braiman & Mathies, 1980; Smith et al., 1985a). The sample (2 OD/cm at 570 nm) was recirculated from a 20-mL reservoir through a glass capillary (0.8-mm diameter) at 400 cm/s. The photocycle was initiated with an ~250–300-mW, cylindrically focused, 514.5-nm pump beam placed upstream from the probe beam. The photoalteration parameter of the pump beam was ~1 (Mathies et al., 1976) with a quantum yield of 0.6 and an extinction coefficient of 35 000 M^{-1} cm^{-1}. Raman spectra were taken with an ~8–10-mW probe beam at 406.7 nm having a photoalteration parameter less than 0.1, assuming a quantum yield of unity. Resonance Raman spectra of BR_{568} and BR_{555} were obtained by using the usual rapid-flow techniques (Smith et al., 1987a,b).

Raman data were acquired by using a Spex 1401 double monochromator with photon counting electronics interfaced to a PDP 11/23 computer. The monochromator was stepped in 2-cm^{-1} increments with a dwell time of 2 s/point. The spectral bandpass was 4 cm^{-1}. Raman spectra were calibrated against the 981.5-cm^{-1} symmetric stretch of sulfate. Typically five to seven scans were needed to give the desired signal-to-noise ratio.

Computational Methods. Normal mode calculations were performed by using the Wilson FG (Wilson et al., 1955) and QCFF/π (Warshel & Karplus, 1974) methods. In all calculations, the chromophore was simplified by replacing carbons 1, 4, and 18 of the ionone ring and the δ carbon of lysine with R groups, having a mass of 15 and the parameters of an sp^3 carbon. FG calculations for BR_{568} and BR_{555} used the geometry and force field from Smith et al. (1987a,b). FG calculations for the 13-cis Schiff bases used the nearly planar geometry generated by QCFF/π. The FG force fields for 13-cis,15-anti and 13-cis,15-syn unprotonated Schiff bases were derived from the all-trans,15-anti protonated Schiff base force field developed by Smith et al. (1985b). The modifications introduced for the unprotonated Schiff base group were as follows [notation as in Smith et al. (1987a)]: K(C=N), 8.25 mdyn/Å^2; K(N—C_{Lys}), 3.9; H(C-C=N), 0.57 (mdyn·Å)/rad^2; H(C=N-C), 0.70; H(N-C-R), 0.69; H(N-CH), 0.389; H(N=CH), 0.191. These values were extracted from the F matrix of a QCFF/π calculation on an all-trans,15-anti unprotonated Schiff base. The force constant changes for the 13-cis geometry were taken from calculations on BR_{555} (Smith et al., 1987b): h($C_{12}C_{13}C_{14}$,$C_{13}C_{14}$H), 0.06 (mdyn·Å)/rad^2; h($C_{12}C_{13}C_{14}$,$C_{13}C_{14}C_{15}$), 0.17; h($C_{20}C_{13}C_{14}$,$C_{13}C_{14}$H), −0.026; h($C_{20}C_{13}C_{14}$,$C_{13}C_{14}C_{15}$), 0.04; m(str,bend), ±0.07 mdyn/rad. The stretch–bend interaction is positive for trans/anti substituents and negative for cis/syn. Force constant changes for the 15-syn geometry were also taken from calculations on BR_{555} (Smith et al., 1987b); H(C=N—C), 0.570; h($C_{14}C_{15}$N,C_{15}NC_{Lys}), 0.17.

Results

Vibrational Properties of Syn and Anti Schiff Bases. The configuration of the protonated Schiff base chromophores in BR_{568} and BR_{555} has been determined by using resonance Raman and solid-state NMR (Smith et al., 1984; Harbison et al., 1984). The Raman method relies on the geometry-sensitive coupling between the C_{14}–C_{15} stretch and the NH rock. The absence of a Schiff base proton in M_{412} precludes the use of this method. However, the C_{15}–H rock and the N–C_{Lys} stretch have the same geometric relationship in the Schiff base as the NH rock and C_{14}–C_{15} stretch in the protonated Schiff base. This suggests that the coupling between the C_{15}—H rock and the N—C_{Lys} stretch may be useful in determining the C=N configuration of unprotonated Schiff base chromophores.

The most convenient way to examine the interaction of the C_{15}–H rock with the N–C_{Lys} stretch is to study 15-deuterio derivatives. Selectively deuterating the C_{15} position shifts the C_{15}–D rocking mode into a clean spectral region where its frequency and normal mode character can be easily analyzed. Also, the C_{15}–D rock is more sensitive to coupling with the N–C_{Lys} stretch, whose frequency is expected in the 1000-cm^{-1} region. Figure 1 presents model calculations to illustrate the sensitivity of the C_{15}—D rock to C=N isomerization. For the anti geometry, the C_{15}–D rock is found at 974 cm^{-1}, and the N-C_{lys} stretch is found at 1050 cm^{-1}. The mass-weighted displacements clearly show that there is little coupling between these two coordinates as indicated by the lack of N–C_{Lys} stretch character in the C_{15}–D rocking mode and vice versa. For the syn geometry, there is much more coupling between the C_{15}–D rock and N–C_{lys} stretch. This is evidenced by the 60 cm^{-1} larger splitting between the modes and the obvious mixing of C_{15}–D rock and N–C_{Lys} stretch character into both

Table I: Wilson FG Normal Modes and Isotopic Frequency Shifts

geometry	frequency (cm^{-1})	description[a]	14,15-^{13}C,15D[b]	ϵ-$^{13}C_{Lys}$,15D[b]
all-trans,15-anti PSB	1050	0.19 (15D) − 0.31 (N–C_{Lys}) + 0.07 (14–15)	1048 (−2)	1038 (−12)
	980	0.76 (15D) + 0.10 (N–C_{Lys}) + 0.07 (14–15)	974 (−6)	979 (−1)
13-cis,15-syn PSB	1068	0.68 (15D) + 0.18 (N–C_{Lys}) + 0.11 (14–15)	1058 (−10)	1064 (−4)
	960	0.36 (15D) − 0.23 (N–C_{Lys}) − 0.02 (14–15)	958 (−2)	951 (−9)
13-cis,15-anti SB	1092	0.09 (15D) − 0.29 (N–C_{Lys}) + 0.03 (14–15)	1089 (−3)	1083 (−9)
	969	0.82 (15D) + 0.03 (N–C_{Lys}) + 0.06 (14–15)	962 (−7)	969 (0)
13-cis,15-syn SB	1062	0.32 (15D) + 0.19 (N–C_{Lys}) + 0.18 (14–15)	1046 (−16)	1057 (−5)
	929	0.64 (15D) − 0.13 (N–C_{Lys}) − 0.004 (14–15)	926 (−3)	925 (−4)

[a] Coefficients (dS/dQ) of symmetry coordinates S in the normal modes Q. Only C_{15}–D rock, N–C_{Lys} stretch, and C_{14}–C_{15} stretch contributions are listed. [b] Frequencies of the calculated normal modes for the indicated isotopic derivatives. Shifts from the unsubstituted molecule are in parentheses.

Table II: QCFF/π Normal Modes and Isotopic Frequency Shifts

geometry	frequency (cm^{-1})	description[a]	14,15-^{13}C,15D[b]	ϵ-$^{13}C_{Lys}$,15D[b]
all-trans,15-anti PSB	1150	0.01 (15D) − 0.31 (N–C_{Lys}) + 0.08 (14–15)	1145 (−5)	1136 (−14)
	994	0.86 (15D) + 0.03 (N–C_{Lys}) + 0.06 (14–15)	988 (−6)	994 (0)
13-cis,15-syn PSB	1092	0.38 (15D) + 0.17 (N–C_{Lys}) + 0.18 (14–15)	1074 (−18)	1087 (−5)
	906	0.48 (15D) − 0.10 (N–C_{Lys}) + 0.01 (14–15)	905 (−1)	902 (−4)
13-cis,15-anti SB	1115	0.01 (15D) − 0.30 (N–C_{Lys}) + 0.05 (14–15)	1110 (−5)	1104 (−11)
	995	0.68 (15D) + 0.02 (N–C_{Lys}) + 0.06 (14–15)	988 (−7)	995 (0)
13-cis,15-syn SB	1062	0.42 (15D) + 0.16 (N–C_{Lys}) + 0.17 (14–15)	1047 (−15)	1058 (−4)
	893	0.51 (15D) − 0.11 (N–C_{Lys}) − 0.02 (14–15)	890 (−3)	889 (−4)

[a] Coefficients (dS/dQ) of symmetry coordinates S in the normal modes Q. Only C_{15}–D rock, N–C_{Lys} stretch, and C_{14}–C_{15} stretch contributions are listed. [b] Frequencies of the calculated normal modes for the indicated isotopic derivatives. Shifts from the unsubstituted molecule are in parentheses.

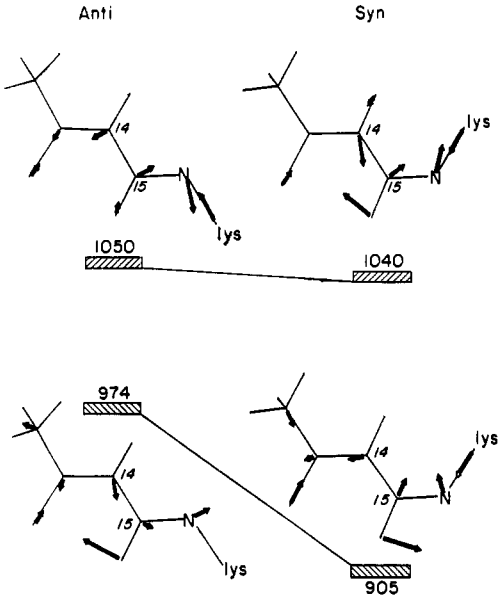

FIGURE 1: Mass-weighted Cartesian displacements of N—C_{Lys} stretching and C_{15}—D rocking normal modes for C=N-anti (left) and C=N-syn (right) unprotonated Schiff bases. The anti Schiff base exhibits relatively localized C_{15}–D rocking and N–C_{Lys} stretching modes at 974 and 1050 cm^{-1}, respectively. These coordinates are strongly mixed in the normal modes of the syn Schiff base. The geometry and vibrational modes were calculated by the QCFF/π method.

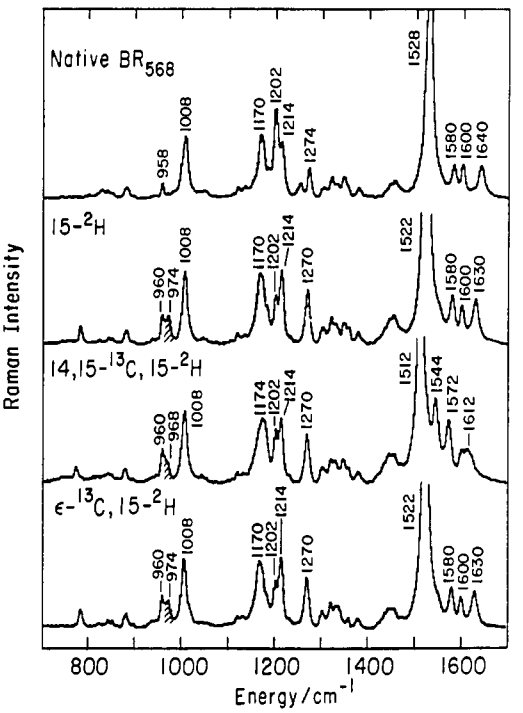

FIGURE 2: Resonance Raman spectra of native, [15-D]-, [14,15-^{13}C,15-D]-, and [ϵ-$^{13}C_{Lys}$,15-D]BR_{568}. Spectra were obtained with a 5-mW, 514.5-nm probe beam cylindrically focused on a flowing (~400 cm/s) stream of purple membrane in 200 mM NaCl and 10 mM phosphate at pH 7 and 22 °C.

modes to form in-phase (1040 cm^{-1}) and out-of-phase (905 cm^{-1}) combinations.

To test the above predictions on the full chromophore, we examined the C_{15}—D rocking mode in BR_{568} (C=N-anti) and BR_{555} (C=N-syn). In BR_{568}, the C_{15}–D rock appears at 974 cm^{-1} (Figure 2); however, in BR_{555} this line shows up at 1047 cm^{-1} (Figure 3). To understand this in more detail, we examined the normal mode analyses of BR_{568} and BR_{555} (Smith et al., 1987a,b). Table I shows that a localized C_{15}–D rocking mode is calculated at 980 cm^{-1} for BR_{568}, consistent with the 974-cm^{-1} experimental value. Also, a localized N–C_{Lys} stretch is calculated at 1050 cm^{-1}, consistent with the N–C_{Lys} stretch assignment made by McMaster and Lewis (1988). The N–C_{Lys} bond is not conjugated with the polyene chain, so a localized N–C_{Lys} stretching mode should have little resonance Raman intensity. For [15-D]BR_{555}, two highly mixed modes are calculated at 1068 and 960 cm^{-1}, which are in-phase and out-of-phase combinations of the C_{15}–D rock and N–C_{Lys} stretch. Only the high-frequency in-phase mode is observed at 1047 cm^{-1}. The high-frequency mode contains significant C_{14}–C_{15} stretch character, while the 960-cm^{-1} mode has little. This suggests that the higher frequency in-phase mode should carry the majority of the resonance Raman intensity, in agreement with experiment. This same pattern of normal mode frequencies and character is seen in the QCFF/π normal

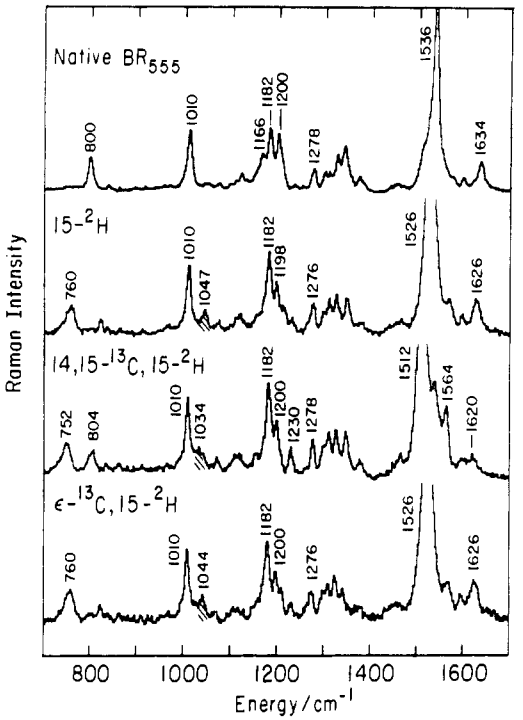

FIGURE 3: Resonance Raman spectra of native, [15-D]-, [14,15-^{13}C,15-D]-, and [ϵ-$^{13}C_{Lys}$,15-D]BR_{555}. Spectra were obtained with a 1–3-mW, 514.5-nm probe beam cylindrically focused on a flowing stream of purple membrane in 200 mM NaCl and 10 mM phosphate at pH 7 and 30 °C.

mode calculations in Table II. This demonstrates that the C_{15}–D rock/N–C_{Lys} stretch coupling pattern does not depend on the details of the force field.

Wilson FG and QCFF/π normal mode calculations were also performed on 13-cis,15-syn and 13-cis,15-anti unprotonated Schiff bases to simulate the possible chromophore geometries of M_{412} and to determine whether the characteristic C_{15}—D rock/N—C_{Lys} stretch coupling pattern is sensitive to the Schiff base protonation state or C_{13}=C_{14} isomerization. The force field used in these calculations was a modified version of the force field for the all-trans protonated Schiff base developed by Smith et al. (1985b). In the 13-cis,15-anti Schiff base calculation (Table I), the C_{15}–D rock and N–C_{Lys} stretch couple weakly, producing a 969-cm^{-1} mode that contains almost entirely C_{15}–D rock character and very little N–C_{Lys} stretch character. The 1092-cm^{-1} mode contains almost all of the N–C_{Lys} stretch character. In the C=N-syn calculation, the C_{15}—D rock and N—C_{Lys} stretch couple strongly. The 1062-cm^{-1} mode is an in-phase mixture of the C_{15}–D rock and N–C_{Lys} stretch with substantial C_{14}–C_{15} stretch character. The 929-cm^{-1} mode is an out-of-phase combination of the C_{15}–D rock and N–C_{Lys} stretch. This same C_{15}–D rock/N–C_{Lys} stretch coupling pattern is seen in the QCFF/π calculations in Table II. Localized C_{15}–D rocking and N–C_{Lys} stretching modes are calculated at 995 and 1115 cm^{-1}, respectively, for the anti geometry. In-phase and out-of-phase combinations of C_{15}–D rock and N–C_{Lys} stretch are calculated at 1062 and 893 cm^{-1}, respectively, for the syn geometry. These FG and QCFF/π calculations indicate that the pattern of C_{15}—D rock frequencies is sensitive primarily to C=N configuration and not to the Schiff base protonation state or the C_{13}=C_{14} configuration.

Experimental Determination of C=N Configuration in M_{412}. To determine the C=N configuration in M_{412}, we must first assign the C_{15}—D rocking mode and then characterize its vibrational properties. The isotopic derivative spectra of

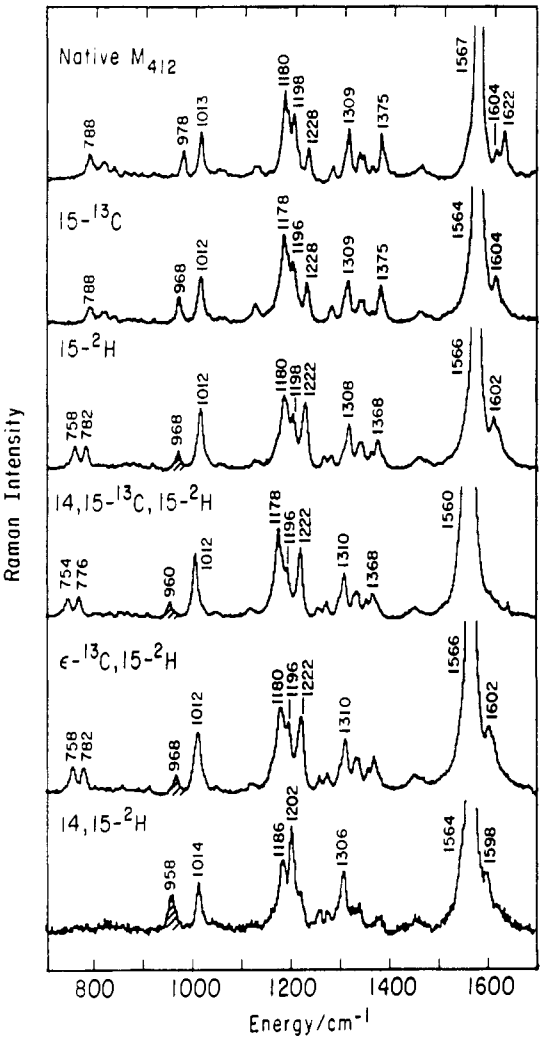

FIGURE 4: Resonance Raman spectra of native M_{412} and its 15-^{13}C, 15-D, 14,15-^{13}C,15-D, ϵ-$^{13}C_{Lys}$,15-D, and 14,15-D_2 derivatives. The photocycle was initiated by an ~300-mW, 514.5-nm pump beam cylindrically focused on a flowing stream (~400 cm/s) of purple membrane in 200 mM NaCl and 10 mM phosphate at pH 7 and 22 °C. The 8–10-mW, 406.7-nm cylindrically focused probe beam was positioned ~0.2 cm (~0.5 ms) downstream.

M_{412} are presented in Figure 4. The native M_{412} spectrum has a strong line at 978 cm^{-1} that is assigned as the C_{15}–H out-of-plane wagging mode based on its 10-cm^{-1} downshift upon ^{13}C substitution at position 15 (12 cm^{-1} calculated). In the [15-D]M_{412} Raman spectrum, a new line appears at 758 cm^{-1}, which must be the downshifted C_{15}–D wag. The remaining line at 968 cm^{-1} in the 15-D derivative can be assigned to the C_{15}–D rock that has shifted into this region from ~1400 cm^{-1}. The 8-cm^{-1} downshift of this line in the 14,15-^{13}C,15-D derivative is within 1 cm^{-1} of the shift calculated for the 13-cis,15-anti Schiff base (Tables I and II). For the 13-cis,15-syn Schiff base geometry, a significantly larger 15–16-cm^{-1} downshift is expected (Tables I and II). The calculated and observed isotopic shifts for BR_{568} and BR_{555} are consistent with this analysis. In [14,15-^{13}C,15-D]BR_{568} (Figure 1), the C_{15}–D rocking mode shifts down by 6 cm^{-1} (6 cm^{-1} calculated). In [14,15-^{13}C,15-D]BR_{555} (Figure 2), the 1047-cm^{-1} mode shifts down 13 cm^{-1} (10 cm^{-1} calculated). The frequency shift observed in [14,15-^{13}C,15-D]M_{412} closely matches that predicted for the anti geometry and confirms the assignment of the 968-cm^{-1} line as the C_{15}–D rocking mode.

The amount of N–C_{Lys} stretch character in the C_{15}–D rocking mode also provides a way of testing our assignments. The calculations for the ϵ-$^{13}C_{Lys}$,15-D derivatives predict

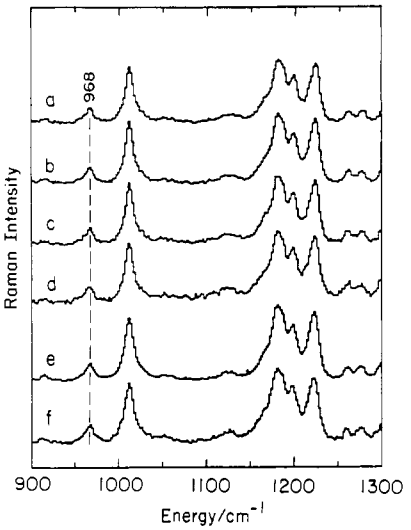

FIGURE 5: Time-resolved resonance Raman spectra of [15-D]M_{412} using a dual-beam, rapid-flow apparatus under various conditions at 22 °C. (a) Fast rise: pH 10, 0.2 M NaCl, and 0.2-ms delay time. (b) Slow rise: pH 7, 0.2 M NaCl, and 0.2-ms delay time. (c) Fast decay: pH 9.1, 0.2 M NaCl, and 0.5-ms delay time. (d) Slow decay: pH 9.1, 0.2 M NaCl, and 5.5-ms delay time. (e) High-salt fast-decay component: pH 9.5, 3 M KCl, and 0.5 ms. (f) High-salt slow-decay component: pH 9.5, 3 M KCl, and 50 ms.

$\leq$1-cm^{-1} shift for the localized C_{15}–D rocking mode in the anti geometry; however, both the in-phase and out-of-phase C_{15}–D rock/N–C_{Lys} stretch modes are calculated to shift 3–6 cm^{-1} for the syn geometry. The resonance Raman spectra of [ϵ-^{13}C,15-D]BR_{568} and BR_{555} provide an experimental confirmation of this prediction. The 1047-cm^{-1} mode in BR_{555} downshifts 3 cm^{-1} in the ϵ-$^{13}C_{Lys}$,15-D derivative, while the 974-cm^{-1} C_{15}–D rocking mode in BR_{568} does not shift (Figures 2 and 3). The 968-cm^{-1} C_{15}–D rocking mode of M_{412} does not shift in the ϵ-$^{13}C_{Lys}$,15-D derivative (Figure 4). This indicates that the 968-cm^{-1} C_{15}–D rocking mode has very little N–C_{Lys} stretch character, supporting the C=N-anti geometry for the chromophore in M_{412}.

A number of studies have indicated that the rise and decay of M_{412} is biphasic (Deng et al., 1985; Hanamoto et al., 1984; Li et al., 1984). This raises the possibility that there are different structural forms of M_{412} (Smith et al., 1989; Kouyama et al., 1988). Therefore, we measured time-resolved resonance Raman spectra of [15-D]M_{412} using a variety of conditions to isolate the different kinetic components (Figure 5). First we used the conditions reported by Deng et al. (1985) to probe the different kinetic components of M observed during flash photolysis: pH 7, 0.2 M NaCl, and 0.2-ms delay time for the slow-rise component and pH 10, 0.2 M NaCl, and 0.2 ms for the fast-rise component (Hanamoto et al., 1984); pH 9.1, 0.2 M NaCl, and 0.5 ms for the fast-decay component and pH 9.1, 0.2 M NaCl, and 5.5 ms for the slow-decay component (Li et al., 1984). Under these conditions we observe no spectral change in the [15-D]M_{412} resonance Raman spectra. This indicates that all the kinetic components of M_{412} reported by the flash photolysis studies have the same C=N-anti configuration.

We also measured time-resolved resonance Raman spectra of [15-D]M_{412} in high salt (3 M KCl) and high pH (pH 9.5). Under these conditions, which enhance the biphasic character of the M_{412} decay, the M_{412} decay can be fit to a biexponential expression with half-times of 1.6 and 120 ms (Fodor et al., 1988b). [15-D]M_{412} resonance Raman spectra were measured at delay times ranging from 0.5 to 50 ms to isolate the fast- and slow-decay components, respectively (Figure 5e,f). No spectral changes were observed, indicating that both the fast and slow M_{412} decay components in the light-adapted photocycle are C=N-anti.

Determination of C_{14}–C_{15} Conformation in M_{412}. To determine the C_{14}–C_{15} conformation in M_{412}, we measured the frequency of the symmetric combination of the C_{14}–D and C_{15}–D rocks. In the 14-s-trans conformation, the symmetric combination of C_{14}–D and C_{15}–D rocks is found at $\sim$970 cm^{-1}, and in the 14-s-cis conformation, the symmetric combination of C_{14}–D and C_{15}–D rocks is calculated at $\sim$850 cm^{-1} (Fodor et al., 1988a). The symmetric combination of C_{14}–D and C_{15}–D rocks in M_{412} is found at 958 cm^{-1} (Figure 4). We conclude that M_{412} contains a 14-s-trans chromophore.

Discussion

The major goal of this study was to develop a method for determining the C=N configuration of the unprotonated Schiff base chromophore in M_{412}. Normal mode calculations on 13-*cis*-retinal Schiff bases show that the C_{15}–D rock/N–C_{Lys} stretch coupling is strong for the syn geometry and weak for the anti geometry. For the 13-cis,15-anti Schiff base, a localized C_{15}–D rocking mode is calculated at $\sim$980 cm^{-1}. For the 13-cis,15-syn Schiff base, two highly mixed modes containing in-phase and out-of-phase combinations of C_{15}–D rock and N–C_{Lys} stretch are calculated at $\sim$1060 and $\sim$910 cm^{-1}, respectively. Resonance Raman spectra of BR_{568} and BR_{555} and our normal mode calculations indicate that (1) the $\sim$980-cm^{-1} mode contains the dominant intensity for the anti geometry, while the $\sim$1060-cm^{-1} mode has the most intensity for the syn geometry, and (2) this pattern is insensitive to the protonation state of the Schiff base and the C_{13}=C_{14} configuration. The [15-D]M_{412} pigment exhibits a mode at 968 cm^{-1} that is assigned as a localized C_{15}–D rock on the basis of the isotopic shifts observed in the ϵ-^{13}C,15-D and 14,15-^{13}C,15-D derivatives. The frequency of this mode, its intensity and isotopic shifts all support the anti geometry and are inconsistent with the syn geometry. Thus, the Schiff base geometry in M_{412} is anti. In addition, the 958-cm^{-1} symmetric combination of C_{14}–D and C_{15}–D rocks demonstrates that M_{412} contains a 14-s-trans chromophore.

Flash photolysis studies show that M_{412} exhibits biphasic formation and decay (Hanamoto et al., 1984; Hess & Kuschmitz, 1977; Li et al., 1984; Ohno et al., 1981; Ort & Parson, 1978). This suggests that different forms of M_{412} exist during the rise and decay of M_{412}. The fast and slow rise and decay components are sensitive to pH (Hanamoto et al., 1984; Li et al., 1984) and ionic strength (Eisenback et al., 1976; Corcoran et al., 1986). Our time-resolved resonance Raman spectra indicate that all the observed forms of M_{412} have a C=N-anti configuration. Thus, changes in C=N configuration cannot be the cause of the biphasic kinetic behavior.

Kinetic studies by Kouyama et al. (1988) suggest that the slow-decaying form of M is produced by the photolysis of N. However, the biphasic decay of M_{412} observed in the time-resolved resonance Raman experiments reported here and by Fodor et al. (1988b) cannot be the result of the photolysis of N. In these experiments, the pump beam photolyzes *only* BR_{568} since the transit time for the sample through the pump beam is short compared with the formation time of N. Also, the recirculation time is $\sim$7 s, which is longer than the decay of N. Thus, our data do not tell us about the chromophore structure of any photolysis products of N.

Recent solid-state NMR studies on M_{412} observed two different M species: a 13-cis,15-anti form and a 13-cis,15-syn form (Smith et al., 1989). The syn form was trapped by continuous illumination (λ > 530 nm) of a sample at pH 10,

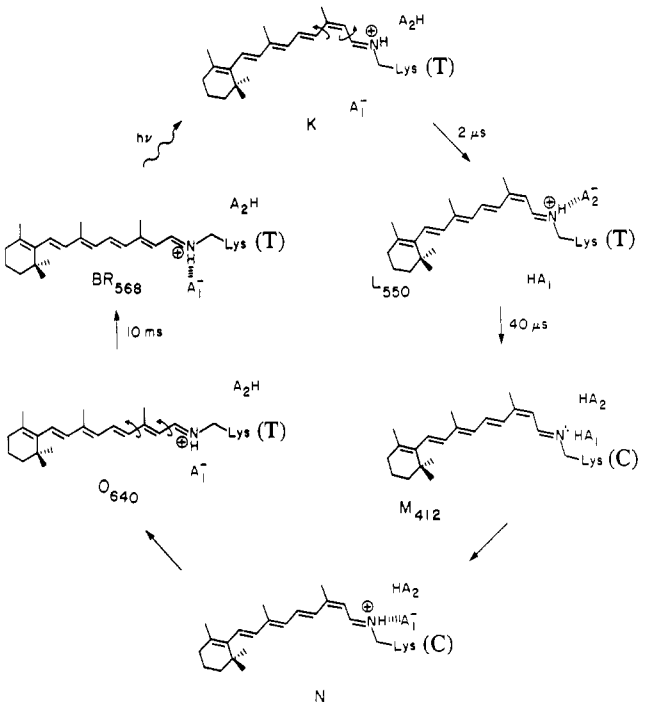

FIGURE 6: Chromophore structure in the intermediates of the bacteriorhodopsin photocycle. The figure also presents a schematic of the C-T model for the proton pump (Fodor et al., 1988b). The *all-trans*-BR_{568} chromophore in the T-protein state photoisomerizes about the C_{13}=C_{14} bond, forming K. The 13-cis chromophore deprotonates during the $L_{550} \rightarrow M_{412}$ transition, and this is accompanied by a protein conformational change (T → C) that disconnects the Schiff base from a residue associated with the exterior (A_2) and connects it to a residue associated with the cytoplasm (A_1). The chromophore reprotonates by accepting a proton from HA_1 in the $M_{412} \rightarrow N$ step. The $N \rightarrow O_{640}$ transition involves thermal reisomerization about the C_{13}=C_{14} bond as well as reversal of the protein conformational change (C → T), which provides the driving force for the reisomerization.

low salt (0.2 M NaCl), and low temperature (−40 °C). The anti form was similarly trapped by constant illumination of a sample in guanidine hydrochloride, alkaline pH, and low temperature (−40 °C). Since our results demonstrate that the structure of M_{412} in the light-adapted photocycle is 13-cis,15-anti, it is reasonable to infer that the guanidine hydrochloride trapping procedure used by Smith et al. (1989) stabilized the more native form of M_{412}.

The structure of the retinal chromophore in every photocycle intermediate is now known, and these results are summarized in Figure 6. BR_{568} contains a 6-s-trans,13-trans,14-s-trans,15-anti PSB chromophore (Smith et al., 1984, 1987a; Harbison et al., 1984, 1985). K_{625} contains a 13-cis,14-s-trans,15-anti PSB (Braiman & Mathies, 1982; Smith et al., 1984, 1985a, 1986). L_{550} contains a 13-cis,14-s-trans,15-anti PSB (Smith et al., 1984, 1985a, 1986; Fodor et al., 1988a). M_{412} contains a 13-cis,14-s-trans,15-anti Schiff base (this work; Braiman & Mathies, 1980; Smith et al., 1985a, 1989). N contains a 13-cis,14-s-trans,15-anti PSB (Fodor et al., 1988b), and O_{640} contains a 13-trans,14-s-trans,15-anti PSB (Smith et al., 1983, 1984, 1985a). It is now clear that the structural events in the photocycle are photoisomerization about the C_{13}=C_{14} bond ($BR_{568} \rightarrow$ J), deprotonation of the Schiff base ($L_{550} \rightarrow M_{412}$), reprotonation of the Schiff base ($M_{412} \rightarrow$ N), and thermal reisomerization about the C_{13}=C_{14} bond ($N \rightarrow O_{640}$).

Figure 6 also presents the C-T model for the mechanism of the proton pump (Fodor et al., 1988b). The ground state consists of the *all-trans*-BR_{568} chromophore with the protein in its T conformation. Light absorption causes a rapid photoisomerization about the C_{13}=C_{14} bond that translates the Schiff base moiety from A_1^- to a new environment near HA_2. The 13-cis chromophore conformationally relaxes and forms a stronger hydrogen bond with A_2^- during the $K \rightarrow L_{550}$ transition. During the $L_{550} \rightarrow M_{412}$ transition, the chromophore deprotonates and the protein changes its conformation from T to C. This conformational change is driven by the presence of the 13-cis chromophore in the active site. The T → C transition shifts a residue connected to the exterior (HA_2) away from the Schiff base and connects the Schiff base with a residue associated with the interior (perhaps HA_1). This conformational change acts as a reprotonation switch that allows reprotonation of the Schiff base by a proton that comes from the cytoplasmic side. Recent Fourier transform infrared studies on site-specific mutants of BR (Braiman et al., 1988a,b) and on isotopically labeled BR proteins (Eisenstein et al., 1987; Engelhard et al., 1985) have identified residues that may be changing protonation state in the photocycle. In particular, Braiman et al. (1988a,b) suggest that A_2 is Asp_{85} and that N is reprotonated by Asp_{212}. The $N \rightarrow O_{640}$ transition involves thermal reisomerization about C_{13}=C_{14} as well as a protein conformational change (C → T). If the C form of the protein has a higher free energy than the T form, this will be a downhill process that stabilizes the 13-trans chromophore. This model does not exclude the possibility of additional states between, for example, L_{550} and M_{412}. However, one important element of the C-T model is the 13-cis,14-s-trans,15-anti structure for M_{412}, which has been demonstrated by the work presented here.

ACKNOWLEDGMENTS

We thank Marcel van der Wielen for helping to prepare [ε-^{13}C]lysine BR. The idea that the C_{15}—D rock/N—C_{Lys} stretch coupling could be used to determine the C=N configuration was developed in discussions with Steve Smith. We also thank Robert Griffin for providing a copy of his manuscript on the solid-state NMR of M_{412} in advance of publication.

REFERENCES

Argade, P. V., Rothschild, K. J., Kawamoto, A. H., Herzfeld, J., & Herlihy, W. C. (1981) *Proc. Natl. Acad. Sci. U.S.A. 78*, 1643–1646.

Braiman, M., & Mathies, R. (1980) *Biochemistry 19*, 5421–5428.

Braiman, M., & Mathies, R. (1982) *Proc. Natl. Acad. Sci. U.S.A. 79*, 403–407.

Braiman, M. S., Mogi, T., Stern, L. J., Hackett, N. R., Chao, B. H., Khorana, H. G., & Rothschild, K. J. (1988a) *Proteins: Struct., Funct., Genet. 3*, 219–229.

Braiman, M. S., Mogi, T., Marti, T., Stern, L. J., Khorana, H. G., & Rothschild, K. J. (1988b) *Biochemistry 27*, 8516–8520.

Corcoran, T. C., Dupuis, P., & El-Sayed, M. A. (1986) *Photochem. Photobiol. 43*, 655–660.

Curry, B., Palings, I., Broek, A. D., Pardoen, J. A., Lugtenburg, J., & Mathies, R. (1985) *Adv. Infrared Raman Spectrosc. 12*, 115–178.

Deng, H., Pande, C., Callender, R. H., & Ebrey, T. G. (1985) *Photochem. Photobiol. 41*, 467–470.

Eisenbach, M., Bakker, E. P., Korenstein, R., & Caplan, S. R. (1976) *FEBS Lett. 71*, 228–232.

Eisenstein, L., Lin, S.-L., Dollinger, G., Odashima, K., Termini, J., Konno, K., Ding, W.-D., & Nakanishi, K. (1987) *J. Am. Chem. Soc. 109*, 6860–6862.

Engelhard, M., Gerwert, K., Hess, B., Kreutz, W., & Siebert, F. (1985) *Biochemistry 24*, 400–407.
Fodor, S. P. A., Pollard, W. T., Gebhard, R., van den Berg, E. M. M., Lugtenburg, J., & Mathies, R. A. (1988a) *Proc. Natl. Acad. Sci. U.S.A. 85*, 2156–2160.
Fodor, S. P. A., Ames, J. B., Gebhard, R., van den Berg, E. M. M., Stoeckenius, W., Lugtenburg, J., & Mathies, R. A. (1988b) *Biochemistry 27*, 7097–7101.
Hanamoto, J. H., Dupuis, P., & El-Sayed, M. A. (1984) *Proc. Natl. Acad. Sci. U.S.A. 81*, 7083–7087.
Harbison, G. S., Smith, S. O., Pardoen, J. A., Winkel, C., Lugtenburg, J., Herzfeld, J., Mathies, R., & Griffin, R. G. (1984) *Proc. Natl. Acad. Sci. U.S.A. 81*, 1706–1709.
Harbison, G. S., Smith, S. O., Pardoen, J. A., Courtin, J. M. L., Lugtenburg, J., Herzfeld, J., Mathies, R. A., & Griffin, R. G. (1985) *Biochemistry 24*, 6955–6962.
Hess, B., & Kuschmitz, D. (1977) *FEBS Lett. 74*, 20–24.
Kouyama, T., Kouyama, A. N., Ikegami, A., Mathew, M. K., & Stoeckenius, W. (1988) *Biochemistry 27*, 5855–5863.
Li, Q. Q., Govindjee, R., & Ebrey, T. G. (1984) *Proc. Natl. Acad. Sci. U.S.A. 81*, 7079–7082.
Mathies, R., Oseroff, A. R., & Stryer, L. (1976) *Proc. Natl. Acad. U.S.A. 73*, 1–5.
Mathies, R. A., Brito Cruz, C. H., Pollard, W. T., & Shank, C. V. (1988) *Science 240*, 777–779.
McMaster, E., & Lewis, A. (1988) *Biochem. Biophys. Res. Commun. 156*, 86–91.
Ohno, K., Takeuchi, Y., & Yoshida, M. (1981) *Photochem. Photobiol. 33*, 573–578.
Ort, D. R., & Parson, W. W. (1978) *J. Biol. Chem. 253*, 6158–6164.
Pardoen, J. A., Winkel, C., Mulder, P. P. J., & Lugtenburg, J. (1984) *Recl. Trav. Chim. Pays-Bas 103*, 135–141.
Scherrer, P., Mathew, M. K., Sperling, W., & Stoeckenius, W. (1989) *Biochemistry 28*, 829–834.
Schulten, K., & Tavan, P. (1978) *Nature (London) 272*, 85–86.
Smith, S. O., Pardoen, J. A., Mulder, P. P. J., Curry, B., Lugtenburg, J., & Mathies, R. (1983) *Biochemistry 22*, 6141–6148.
Smith, S. O., Myers, A. B., Pardoen, J., Winkel, C., Mulder, P. P. J., Lugtenburg, J., & Mathies, R. (1984) *Proc. Natl. Acad. Sci. U.S.A. 81*, 2055–2059.
Smith, S. O., Lugtenburg, J., & Mathies, R. A. (1985a) *J. Membr. Biol. 85*, 95–109.
Smith, S. O., Myers, A. B., Mathies, R. A., Pardoen, J. A., Winkel, C., van den Berg, E. M. M., & Lugtenburg, J. (1985b) *Biophys. J. 47*, 653–664.
Smith, S. O., Hornung, I., van der Steen, R., Pardoen, J., Braiman, M. S., Lugtenburg, J., & Mathies, R. A. (1986) *Proc. Natl. Acad. Sci. U.S.A. 83*, 967–971.
Smith, S. O., Braiman, M. S., Myers, A. B., Pardoen, J. A., Courtin, J. M. L., Winkel, C., Lugtenburg, J., & Mathies, R. A. (1987a) *J. Am. Chem. Soc. 109*, 3108–3125.
Smith, S. O., Pardoen, J. A., Lugtenburg, J., & Mathies, R. A. (1987b) *J. Phys. Chem. 91*, 804–819.
Smith, S. O., Courtin, J., van den Berg, E., Winkel, C., Lugtenburg, J., Herzfeld, J., & Griffin, R. G. (1989) *Biochemistry 28*, 237–243.
Stoeckenius, W., & Bogomolni, R. A. (1982) *Annu. Rev. Biochem. 51*, 587–616.
Warshel, A., & Karplus, M. (1974) *J. Am. Chem. Soc. 96*, 5677–5689.
Wilson, E. B., Decius, J. C., & Cross, P. C. (1955) *Molecular Vibrations*, McGraw-Hill, New York.

Lipid Chains and Cholesterol in Model Membranes: A Monte Carlo Study†

H. L. Scott* and S. Kalaskar‡
Department of Physics, Oklahoma State University, Stillwater, Oklahoma 74078
Received July 29, 1988; Revised Manuscript Received January 30, 1989

ABSTRACT: The Monte Carlo method has been employed to study the equilibrium properties of a planar array of hydrocarbon chains interacting with a cholesterol molecule. The chains are arranged to model one monolayer of a lipid bilayer and within this monolayer are allowed to move laterally and change conformations by gauche rotations. In the simulation cell there are 90 lipid chains and a single cholesterol molecule. Periodic boundary conditions are imposed upon the cell. The primary results of the calculations are order parameter profiles for the C–C bonds. These are calculated for (i) all chains, (ii) the 6 chains which are nearest neighbors to the cholesterol, and (iii) the 12 chains which are next-nearest neighbors to the cholesterol. Calculations are carried out for C-14, C-16, and C-18 chains. The results show that cholesterol strongly affects the upper portions of the chains, leaving them less able to change conformations. For C-16 and C-18 chains, the chain termini of the cholesterol neighbors are more disordered than the bulk chain termini. The magnitude of the effect depends strongly on the chain length. The results suggest that the changes in the lipid phase transition caused by cholesterol are a consequence of each cholesterol hindering the rotameric freedom of five to seven lipid chains.

The role of cholesterol in animal cell membranes (and other sterols in plant cell membranes) has been debated for many years [for a recent review, see Presti (1985)]. On the one hand, calorimetric studies show that cholesterol acts as a "disordering" agent in lipid bilayers in the sense that the otherwise sharp main lipid chain melting phase transition becomes broad and diffuse with increasing cholesterol concentration (Hinz & Sturtevant, 1972; Mabrey et al., 1978; Estep et al., 1978). On the other hand, cholesterol acts as an

†Supported in part by National Science Foundation Grant DMB 8703644.
‡Present address: Department of Chemistry, Utah State University, Logan, UT 84321.

0006-2960/89/0428-3687$01.50/0